

Hypothalamic MCH neuron activity dynamics during cataplexy of narcolepsy

<https://doi.org/10.1523/ENEURO.0017-20.2020>

Cite as: eNeuro 2020; 10.1523/ENEURO.0017-20.2020

Received: 20 January 2020

Revised: 3 March 2020

Accepted: 7 March 2020

This Early Release article has been peer-reviewed and accepted, but has not been through the composition and copyediting processes. The final version may differ slightly in style or formatting and will contain links to any extended data.

Alerts: Sign up at www.eneuro.org/alerts to receive customized email alerts when the fully formatted version of this article is published.

Copyright © 2020 Sun and Liu

This is an open-access article distributed under the terms of the Creative Commons Attribution 4.0 International license, which permits unrestricted use, distribution and reproduction in any medium provided that the original work is properly attributed.

1
2
3
4
5
6
7
8

9
10
11
12
13
14
15
16
17
18
19
20
21
22
23
24
25
26
27
28
29
30
31
32
33

34

35

36

1. **Manuscript Title:** Hypothalamic MCH neuron activity dynamics during cataplexy of narcolepsy

2. **Abbreviated Title:** MCH neurons are silent during cataplexy

3. Author list:

Ying Sun, Department of Psychiatry and Behavioral Sciences, Medical University of South Carolina, Charleston, SC, 29425

Meng Liu, Department of Psychiatry and Behavioral Sciences, Medical University of South Carolina, Charleston, SC, 29425

Author Contributions: Sun Y performed animal surgery, EEG/EMG & Ca²⁺ recording, and data analysis. Liu M performed the data analysis and drafted the manuscript.

5. **Correspondence should be addressed to** Meng Liu, liumen@musc.edu

6. Number of Figures: 2

7. Number of Tables: 1

8. Number of Multimedia: 3

9. Number of words for Abstract: 167

10. Number of words for Significance Statement: 93

11. Number of words for Introduction: 319

12. Number of words for Discussion: 1022

13. Acknowledgment:

We thank Dr. Priyattam Shiromani, Dr. Blanco-Centurion Carlos, Dr. SiWei Luo, and Mr. Aurelio Vidal-Ortiz at the Medical University of South Carolina for advice, guidance, and technical support on animal surgery and calcium imaging data processing. We thank Dr. Jiexiang Li at the College of Charleston for advice on data processing. Supported by NIH grants 1R01NS096151, 1R21NS101469.

14. Conflict of Interest: A (No)

37 **Abstract**

38 Hypothalamic orexin (HCRT) deficiency causes sleep disorder narcolepsy with
39 cataplexy in humans and murine. As another integral group of sleep/wake-regulating
40 neurons in the same brain area, the melanin-concentrating hormone (MCH) neurons'
41 involvement in cataplexy remains ambiguous. Here we used the live animal deep-brain
42 calcium (Ca^{2+}) imaging tool to record MCH neuron dynamics during cataplexy by
43 expressing calcium sensor GCaMP6s into genetically defined MCH neurons in orexin
44 knockout mice, which are a model of human narcolepsy. Similar to wild type mice, MCH
45 neurons of the narcoleptic mice displayed significantly higher Ca^{2+} transient fluorescent
46 intensity during rapid eye movement (REM) sleep and active waking episodes
47 compared to non-rapid eye movement (NREM) sleep. Moreover, MCH neurons
48 displayed significantly lower Ca^{2+} signals during cataplexy. Importantly, a pre-cataplexy
49 elevation of Ca^{2+} signals from MCH neurons was not a prerequisite for cataplexy
50 initiation. Our results demonstrated the inactivation status of MCH neurons during
51 cataplexy and suggested that MCH neurons are not involved in the initiation and
52 maintenance of cataplexy in orexin knockout mice.

53

54 **Significance Statement**

55 The cataplexy of narcolepsy shares many similarities with normal REM sleep. Thus,
56 REM sleep-promoting MCH neurons are thought to be part of the cataplexy circuitry.
57 Suppressing MCH neurons is assumed to block cataplexy. However, we found that
58 MCH neurons were always inactive during cataplexy in orexin knockout mice. Pre-

59 cataplexy activations of MCH neurons were no different from the activation during
60 regular waking episodes. Importantly, cataplexy could occur in the absence of these
61 pre-cataplexy activations. These results suggest that MCH neurons are not a key
62 component of the cataplexy circuitry in orexin knockout mice.

63

64 **Introduction**

65 Orexin (hypocretin, HCRT) and melanin-concentrating hormone (MCH) are
66 hypothalamic neuropeptides regulating sleep and wakefulness. Orexin neurons are
67 wake-active, promoting arousal and maintaining wakefulness (Adamantidis *et al.*, 2007;
68 Alexandre *et al.*, 2013) while MCH neurons are predominantly rapid eye movement
69 (REM) sleep-active and promote REM sleep (Blanco-Centurion *et al.*, 2016; Blanco-
70 Centurion *et al.*, 2019a; Izawa *et al.*, 2019; Jegu *et al.*, 2013; Konadhode *et al.*, 2013).
71 Lack of orexin neurons or loss of the orexin gene causes sleep disorder narcolepsy and
72 its signature symptom cataplexy, a sudden skeletal muscle atonia during waking
73 (Chemelli *et al.*, 1999; Hungs *et al.*, 2001; Lin *et al.*, 1999). Cataplexy or cataplexy-like
74 behavior has not been reported in MCH or its receptor knockout mice, suggesting that
75 there is no causal effect between MCH deficiency and cataplexy. However, whether
76 MCH neurons play a role in cataplexy in narcolepsy patients or narcoleptic animals is
77 still unknown. The question could be answered by manipulating MCH neurons in
78 narcoleptic animals using optogenetic or chemogenetic tools. Indeed, a recent study
79 indicated that chemogenetically activating MCH neurons increased cataplexy and
80 abnormal REM sleep in orexin knockout mice (Naganuma *et al.*, 2018). However, we

81 believe that the instinctive status of MCH neurons during cataplexy is still crucial for
82 understanding the exact involvement of MCH neurons in cataplexy and for designing
83 optimal intervention strategies to block cataplexy. For instance, if MCH neurons are
84 active during cataplexy, further stimulation/excitation may have no noticeable effects
85 due to the “ceiling” effect. Likewise, further inhibition might be ineffective due to the
86 “floor” effect if MCH neurons are already silent during cataplexy. In this study, we took
87 advantage of the novel genetic Ca^{2+} imaging tool to record real-time MCH neuronal
88 activities during spontaneous cataplexy and emotional cataplexy induced by either
89 positive (palatable food: milk) or negative (innate fear: predator odor) emotions. We
90 want to know whether and how MCH neurons contribute to the generation or
91 propagation of cataplexy.

92

93

94 **Materials and Methods**

95 **1. Animals and surgery**

96 All the manipulations done to the mice followed the policies established in the
97 National Institutes of Health Guide for the Care and Use of Laboratory Animals and
98 were approved by the Institutional Animal Care and Use Committee (Protocol # IACUC-
99 2019-00723).

100 To specifically target MCH neurons in narcoleptic mice, orexin KO mice (*Hcrt*^{-/-}) mice
101 (derived from founders donated by Dr. Yanagisawa, Southwestern Medical Center,
102 Dallas, TX) were crossed with MCH-Cre mice (www.jax.org, stock #014099, Bar Harbor,

ME). Offsprings with the confirmed genotype *MCH-Cre^{+/+}/Hcrt^{-/-}* were used as the narcoleptic group (n = 8, both sexes, 6–10 months of age). Genotype validation on mice tail snips was done off-site by Transnetyx (Cordova, TN). The temperature in the mice housing/recording room was always maintained at 23–25°C under a 12 h light/dark cycle (lights on at 6:00 A.M.). Mice were given *ad libitum* access to regular laboratory food and water.

Under deep anesthesia (isoflurane 1.0–2.0%) and using a stereotaxic frame (Kopf, Tujunga, CA), adeno-associated virus (AAV) vectors with Cre-inducible expression of GCaMP6 slow (AAV5-CAG-DIO-GCaMP6s, Titer: 3.48×10^{13} genomic copies/mL; University of Pennsylvania Preclinical Vector Core) were microinjected unilaterally into the lateral hypothalamus at the following coordinates: 1.11 mm posterior to Bregma, 1.25 mm lateral to the sagittal suture, and 4.60 mm ventral to the brain surface (Hof *et al.*, 2000). Viral vectors were delivered in a volume of 500nL using a 10.0 μ L Hamilton syringe coupled to a 33-gauge stainless steel injector (Plastics One, Roanoke, VA). Injections were done gradually over 25 min. After microinjection, the injector needle was left in place for 15 min and then withdrawn slowly. At this time, and following the same injection track, a miniature Gradient Refractive INdex lens (GRIN, outer diameter: 0.6 mm, length: 7.3 mm; Inscopix Inc, Palo Alto, CA) was driven into the brain just above the injection target and cemented to the skull. Then, as described elsewhere (Liu *et al.*, 2011), four small screw-type electrodes and a pair of plate-type electrodes (Plastics One, CA) were implanted onto the mouse skull and nuchal muscles for recording the electroencephalogram (EEG) and electromyogram (EMG) activity respectively. Ten days after the GRIN lens placement, mice were deeply anesthetized again (1.0–2.0%

126 isofluorane). A baseplate was attached to a single photon miniaturized fluorescence
 127 microscope/CCD camera (nVoke from Inscopix, Inc., CA). The miniaturized microscope,
 128 along with the baseplate, were carefully placed atop the GRIN lens. The distance
 129 between the miniaturized microscope and the GRIN lens top was precisely adjusted
 130 until fluorescent neurons came into focus. At this focal point, the baseplate was
 131 secured around the GRIN lens cuff with dental cement, and then the microscope was
 132 detached. To protect the GRIN lens from debris and scratches, a cap was secured onto
 133 the baseplate. One week later, mice were habituated to the recording experiment
 134 setting for three consecutive days before the sleep and Ca^{2+} recording started.

135 **2. Sleep recording and identification of sleep states or cataplexy**

136 After being amplified and filtered (0.3–100 Hz for EEG; 100–1000 Hz for EMG, MP150
 137 system; Biopac Systems Inc., CA), the EEG/EMG signals were acquired and
 138 synchronized to the imaging of the Ca^{2+} transients. In parallel, a night-vision camera
 139 was used to record mouse behavior. Streaming video of the mouse behavior was also
 140 synchronized with the imaging of the Ca^{2+} transients (Neuroscience Studio acquisition
 141 software, Doric Lenses Inc, QC, Canada). NeuroExplorer software (Nex Technologies,
 142 CO, USA) was used to plot the spectrogram of the EEG activity (1 s window size and
 143 0.5 s overlap).

144 The EEG/EMG data (as CSV files) along with synchronized behavior video files were
 145 then transferred to the SleepSign software (KISSEI Comtec Ltd., Nagano, Japan) and
 146 scored in 4 s epochs as wakefulness, non-rapid eye movement (NREM) sleep, rapid
 147 eye movement (REM) sleep, and cataplexy. Wakefulness was identified by the
 148 presence of desynchronized EEG coupled with high amplitude EMG activity. In this

149 study, we focused on active wakefulness (AW) when the mice displayed behaviors such
 150 as walking, rearing, grooming, eating, drinking, digging, and exploring. NREM sleep was
 151 scored when the EEG showed high-amplitude/low-frequency waves (delta waves)
 152 together with a lower EMG activity relative to waking. REM sleep was identified by the
 153 presence of regular EEG theta activity coupled with very low EMG activity.

154 To be qualified as a cataplexy attack, an episode had to meet the following criteria: 1)
 155 An abrupt episode of nuchal atonia lasting at least 8 s, 2) Immobility during the episode,
 156 3) theta activity dominant EEG during the episode, and 4) at least 40 s of wakefulness
 157 preceding the episode (discrete cataplexy) or the first episode when several cataplexy
 158 episodes occur sequentially. The above criteria were slightly modified from the
 159 International Working Group on Rodent Models of Narcolepsy (Scammell *et al.*, 2009).
 160 We also named the 40 s AW episodes preceding the cataplexy as pre-cataplexy AW
 161 episodes to distinguish them from other AW episodes not followed by cataplexy.

162 **3. Miniature microscopy Ca^{2+} transients imaging**

163 At 10:00 A.M., the mouse was gently restrained (swaddled in Terrycloth), while a
 164 dummy miniscope (with the same size and weight as the real miniature fluorescent
 165 microscope) was attached to its baseplate. At the same time, a lightweight cable was
 166 plugged to record the EEG/EMG signals. The tethered mouse was then returned to the
 167 home cage and allowed to adapt for 6 h for three consecutive days. On the fourth day
 168 (the recording day), the same adaptation routine was followed with the real miniscope,
 169 but at 5:00 PM, Ca^{2+} transients-derived fluorescence began to be imaged by the nVoke
 170 miniaturized microscope/CCD camera (Inscopix, CA) and collected by its acquisition
 171 software. Ca^{2+} associated fluorescence was continuously generated by a blue LED

172 (power: 0.2 mW) and imaged at 5 frames per second (fps). To synchronize the
 173 timestamps of the Ca^{2+} imaging with the EEG/EMG, a TTL signal was sent from the
 174 nVoke interface console into the Doric console. After 30 min of undisturbed recording,
 175 the mouse was exposed to milk (whole milk, 2 mL) for 30 min and coyote urine (1 mL,
 176 www.predatorpee.com, Bangor, ME) for 30 min between 5:30 P.M. and 7:00 P.M. (Liu
 177 *et al.*, 2016).

178 **4. Analysis of Ca^{2+} transients imaging data**

179 The Ca^{2+} transient data were processed offline by the Inscopix data processing
 180 software (version 1.1.2). Briefly, raw movies were first pre-processed to correct for
 181 defective pixilation, row noise, and dropped frames. Preprocessed movies were then
 182 corrected for motion artifacts to generate the steadiest Ca^{2+} fluorescent signals. The
 183 motion-corrected movies were subsequently mean filtered. To normalize the Ca^{2+}
 184 signals, a single frame average projection of the filtered movie was generated. The
 185 average frame was used as the background fluorescence (F_0) to calculate the
 186 instantaneous normalized Ca^{2+} fluorescent signals ($\Delta F/F$) according to the formula;
 187 $(\Delta F/F)_i = F_i - F_0 / F_0$ where i represents each movie frame. The normalized movie or “ $\Delta F/F$
 188 movie” was then used for semiautomatic extraction of Ca^{2+} fluorescent signals
 189 associated with individual cells based on the principal and independent component
 190 analysis (PCA-ICA). Regions of interest (ROIs) identified by the PCA-ICA were visually
 191 selected as candidate cells based on $\Delta F/F$ and the image (cell-morphology). To be
 192 chosen as *bona-fide* neurons, Ca^{2+} traces had to fulfill the canonic Ca^{2+} spike waveform
 193 featuring fast-rising onset followed by slower decaying signals. The Ca^{2+} traces ($\Delta F/F$)
 194 of each ROI (cell) were further standardized as Z-scores using the mean and standard

deviation (SD) of each cell's $\Delta F/F$ ($Z\text{-score} = (\Delta F/F - \text{Mean})/SD$). Since the lowest Z-score values in the normal sleep/wake states during the undisturbed recordings were observed in NREM sleep, and no cell reached its maximal activity during NREM sleep, we used the average Z-score of the NREM sleep (Z_{NREM}) as the baseline. If the average Z-score of a cell during a specific state is equal to or greater than ($Z_{\text{NREM}} + 1.0$) during the undisturbed recording period, it was scored as an "ON" cell in that state. We then used the percentage threshold, which was defined as 80% of the maximum Z-score value during the whole recording period, to detect the frequency of the prominent neuronal peak events (per cell, per minute), and we set 2 s as the minimum interval between two adjacent peaks.

5. Histology

At the end of the study, the mice were anesthetized with isoflurane (5%) and perfused transcardially with 0.9% saline (5–10 mL) followed by 10% buffered formalin in 0.1 M PBS (50 mL). Mice brains were harvested and cross-sectioned at 40 μm thickness (four sets) on a compresstome (Precisionary Instruments, Greenville, NC). To visualize the GRIN lens track and the location of the GCaMP6s transgene expression, coronal sections were scanned on a Leica fluorescent microscope. To verify that GCaMP6s was expressed exclusively in MCH neurons, MCH immunostaining was performed on one set of brain sections. Briefly, the sections were incubated at room temperature for 24 h with rabbit anti-MCH polyclonal antibody (1:500 dilutions, Phoenix Pharmaceuticals, Burlingame, CA), followed by 1 h incubation with Alexa fluor-568 donkey anti-rabbit IgG (1:500, Invitrogen, CA). GCaMP6s and MCH positive cells were counted on digitized images. To confirm the correctness of the genotyping, orexin immunostaining was

218 conducted on a separate set of brain sections. Briefly, the sections were incubated at
 219 room temperature for 24 h with goat anti-orexin polyclonal antibody (1:5000 dilutions,
 220 Santa Cruz Biotechnology, CA), followed by 1 h incubation with biotinylated donkey
 221 anti-goat IgG (1:500, Millipore, Burlington, MA) secondary antibody and finally labeled
 222 using ABC–DAB–nickel staining (Vector Laboratories, Burlingame, CA).

223 **6. Statistical analysis**

224 The one-way ANOVA and Bonferroni post-hoc tests (SPSS, version 25) were used to
 225 compare the means of the Z-score values among the sleep/wake states. Statistical
 226 significance was evaluated at the $P < 0.05$ (two-tailed) level (Kirk, 1968).

227

228 **Results**

229 **1. MCH/Orexin immunostaining and GCaMP6s expression**

230 We found that orexin+ neurons were utterly absent in the *MCH-Cre^{+/+}/Hcrt^{-/-}* mice
 231 used in this study, unlike the dense distributions of orexin+ neurons in the lateral
 232 hypothalamus of the wild-type MCH-Cre mice (Figure 1A and 1B). These
 233 immunostaining results, together with the genotyping results and signature cataplexy
 234 behaviors, validated the animal model of narcolepsy. We recorded continuous Ca^{2+}
 235 transient signals from four of the eight mice installed with the GRIN lenses. In these four
 236 mice, GCaMP6s predominantly expressed within the lateral hypothalamus area (Figure
 237 1C and 1D). The MCH immunostaining results showed that approximately 95-98% of
 238 the GCaMP6s expressing neurons also contained MCH in the cytoplasm (Figure 1, D–
 239 F).

240 **2. MCH neuronal activities during undisturbed sleep/wake cycle**

241 Altogether, we imaged 67 MCH neurons from 4 narcoleptic mice (2 males and 2
 242 females). These MCH neurons displayed activity patterns very similar to those of the
 243 wild-type MCH neurons (Blanco-Centurion *et al.*, 2019b) (Figure 2 A and 2B, and Video
 244 1). A marked increase in the average Z-scores was observed during REM sleep and
 245 active waking (AW) when compared to NREM sleep (Figure 2C). The results of the one-
 246 way ANOVA analysis revealed a significant effect on the Ca^{2+} fluorescent intensity $\Delta F/F$
 247 Z-scores ($F_{(6, 468)}=58.38$, $p<0.001$) depending on individual sleep/wake states. The
 248 cells were categorized as ON (activated) cells based on the Ca^{2+} fluorescent intensity
 249 data before exposures to milk or coyote urine. Of the total 67 cells, 59.70% (40/67) were
 250 REM-ON only, 20.90% (14/67) were AW-ON only, 14.93% (10/67) were REM/AW-ON,
 251 and 4.48% (3/67) were unscored (no significant activity change among the different
 252 sleep/wake states was found during the undisturbed recording).

253 **3. MCH neuronal activities during cataplexy and sleep attack**

254 In addition to cataplexy, some narcoleptic mice may present another behavioral
 255 arrest called sleep attack, which is a brief NREM sleep intrusion during AW such as
 256 exploring, grooming, and eating. Sleep attacks were characterized by a mixture of delta
 257 and theta activities in the EEG, in contrast to cataplexy where theta activity dominates.
 258 We recorded 12 cataplexy bouts (3 spontaneous ones before any exposure, 4 after the
 259 milk exposure, and 5 after the odor exposure) and 8 sleep attack bouts (4 before any
 260 exposure, 2 after the milk exposure, and 2 after the odor exposure) during the whole 2-h
 261 recording periods. The average Ca^{2+} intensity levels during cataplexy and sleep attack
 262 were similar to those of the NREM sleep and significantly lower than that of the REM

263 sleep and AW. Importantly, neither “cataplexy-ON” nor “sleep attack-ON” cells were
264 identified during the whole 2-h recording (Figure 2D and 2E, Videos 2 and 3).

265 In the 30 min of undisturbed (before any exposure) and milk exposure recording,
266 significantly elevated Ca^{2+} signal intensities from MCH neurons could be observed
267 during AW episodes not followed by cataplexy as well as AW episodes closely followed
268 by a cataplexy bout (we named these episodes as pre-cataplexy AW episodes). The
269 increased Ca^{2+} signal during these pre-cataplexy AW episodes suddenly dropped to the
270 basal level once the cataplexy began (Figure 2D and 2E). Upon the predator odor
271 (coyote urine) exposure, the mice showed several typical behavioral signs of fear,
272 including exploration, avoidance, and escape attempts. However, the Ca^{2+} signal
273 intensities from MCH neurons showed insignificant increases during these fear
274 response behaviors. In the meantime, sleep attack or cataplexy continued to be
275 observed, during which time MCH neurons continued to display low Ca^{2+} fluorescent
276 intensities (Figure 2E, Video 3).

277 To better understand the nature of the Ca^{2+} signal elevation during the pre-
278 cataplexy episodes (except the AW episodes after predator odor exposure), we
279 compared the Ca^{2+} signal intensities (average Z-scores) and peak frequencies between
280 the pre-cataplexy AW episodes (Pre-C AW) and the AW episodes not followed by
281 cataplexy (N-C AW), but we found no significant difference (Figure 2F). Furthermore,
282 we found that the sources or components of the Pre-C AW-ON cells and N-C AW-ON
283 cells are very similar (Table 1). We did not find any significant difference between these
284 two types of AW episodes.

285

286 Discussion

287 Cataplexy, presented as a sudden skeletal muscle paralysis or weakness during
288 waking, is the most disabling symptom of sleep disorder narcolepsy (Reading, 2019). In
289 murine models of narcolepsy, cataplexy usually occurs during the active waking status
290 of the animal, such as running, exploring, grooming, or responding to emotion stimuli
291 (Morawska *et al.*, 2011; Overeem *et al.*, 2001; Reading, 2019). The brain circuitry
292 responsible for cataplexy is not completely clear. Using the novel calcium imaging tool,
293 we previously identified that the amygdala neuronal hyperactivity is associated with
294 emotional cataplexy (Sun *et al.*, 2019). In the present study, we recorded the *in vivo*
295 activities of individual MCH neurons during cataplexy using the same methodology. We
296 found that the majority of the recorded MCH neurons in the narcoleptic mice were most
297 active during REM sleep, which is very similar to what occurs in wild-type mice (Blanco-
298 Centurion *et al.*, 2019b; Izawa *et al.*, 2019). Some recorded MCH neurons were also
299 active during exploring, eating, and milk drinking, which is compatible with prior
300 research about the effects of MCH neurons on food intake (Dilsiz *et al.*, 2019; Gonzalez
301 *et al.*, 2016). Although prior studies indicated that MCH may regulate stress or fear
302 (Carlini *et al.*, 2006; Roy *et al.*, 2006), we did not observe overt MCH neuron activation
303 during the innate fear coyote urine exposure, implicating that the MCH neurons that
304 were usually active during active waking were suppressed by fear in the narcoleptic
305 mice. Further research on wild-type mice MCH neurons is need to explore the exact
306 correlation between MCH neurons and fear regulation.

307 Nevertheless, our results demonstrated that MCH neurons always stayed inactive
308 during both spontaneous and emotional cataplexy (induced by milk or coyote urine),

309 indicating that MCH neuron activation is not necessary for maintaining cataplexy in
310 orexin knockout mice. Although MCH neuron activation was observed in some pre-
311 cataplexy episodes, the activation intensity, pattern, and “ON” cell components were
312 very similar to the activation noted in the regular active waking episodes. In contrast to
313 the amygdala GABAergic neurons that displayed abnormal hyperactivity and increased
314 activated cell numbers during the pre-cataplexy episodes that were followed by the
315 coyote urine-induced cataplexy (Sun *et al.*, 2019), neither hyperactivity nor recruitment
316 of more REM-ON MCH cells has been found in these pre-cataplexy MCH neuron
317 activations. This implicates that the pre-cataplexy activations are nothing different from
318 the activations during regular active waking. Noticeably, some cataplexy bouts could
319 happen even when the MCH neuron activation was absent (Figure 2E). All this
320 evidence indicates that MCH neuron activation during the pre-cataplexy episodes might
321 be unnecessary for or irrelevant to cataplexy triggering. A previous study reported
322 activated MCH neurons during cataplexy by examining c-Fos and MCH double-labeled
323 neurons (Oishi *et al.*, 2013). However, the c-Fos expression is an indirect marker of
324 neuronal activation and lacks temporal and spatial specificities. There is a possibility
325 that c-Fos expression induced by the active waking behaviors immediately before
326 cataplexy is mistaken as having been induced by cataplexy. Our work provides the first
327 direct evidence of phenotype-and cataplexy-specific neuronal activities associated with
328 MCH neurons.

329 Cataplexy is the most disabling feature in narcolepsy patients. Due to the
330 similarities of the EEG spectrum and muscle atonia features, cataplexy has long been
331 considered as a REM sleep intrusion into waking or abnormal REM sleep during waking

(Luppi *et al.*, 2011; Roth *et al.*, 1969). Indeed, studies have found that cataplexy and REM sleep share some common neural substrates (Dauvilliers *et al.*, 2014; Peever *et al.*, 2016; Thakkar *et al.*, 1999). Thus, MCH neurons, an important REM sleep-regulating hub, are thought to trigger intrusions of REM sleep bouts into waking in the absence of orexin, consequently resulting in cataplexy. In support of this hypothesis, chemogenetic activation of MCH neurons increased cataplexy and abnormal REM sleep (Naganuma *et al.*, 2018). However, some emerging evidence is not supportive of this hypothesis. For instance, stimulating cholinergic in the basal forebrain of narcoleptic dogs induced cataplexy attacks but did not block the cyclicity of burst of rapid eye movement, implying that separate mechanisms underlie cataplexy and REM sleep (Nishino *et al.*, 2000). MCH neuron activation is highly correlated with REM sleep in normal mice, while we found an explicit disassociation between MCH activation and cataplexy. The above evidence suggests that cataplexy and REM sleep might have discrete mechanisms and MCH neurons stay outside the cataplexy circuit. However, it does not necessarily exclude the possibility that MCH activation triggers abnormal REM sleep and muscle weakness. In other words, the abnormal REM sleep intrusion or muscle weakness induced by stimulating MCH neurons exogenously is mechanistically distinct from—albeit similar to—the muscle atonia seen in cataplexy of narcolepsy. Moreover, the silence of the MCH neurons during cataplexy implicates that their appropriate activation may inhibit cataplexy. Indeed, a recent study demonstrated that ablating both orexin and MCH neurons worsens cataplexy, revealing the possible role of MCH neurons in preventing cataplexy (Hung *et al.*, 2019).

Notably, unlike in the orexin neuron ablation models for human narcolepsy (Hara *et al.*, 2001; Tabuchi *et al.*, 2014), the original orexin neurons in the orexin knockout mice are still intact despite the loss of orexin peptides. These neurons might affect the activity of MCH neurons via other neuropeptides coexisting with orexin, such as dynorphin (Chou *et al.*, 2001). Thus, a similar calcium imaging study on the orexin neuron ablation model is needed to further confirm our findings.

Sleep attack occurs in some narcoleptic patients and mice. In humans, it takes place when an overwhelming sense of sleepiness comes on quickly and is considered a symbol of excessive daytime sleepiness. In mice, such an attack is manifested as a short NREM sleep intrusion into waking (Hishikawa *et al.*, 1968; Liu *et al.*, 2011). It is probably caused by the increased sleep drive when orexin is missing, or when orexin neurons die. The missing MCH neuron activation supports the NREM sleep mechanism of sleep attacks.

In conclusion, we found that MCH neuron activation is unnecessary for the maintenance and initiation of cataplexy in orexin knockout mice. Thus, MCH neurons might not be one of the crucial nodes in the cataplexy brain circuitry in orexin knockout mice.

Reference

- Adamantidis, A. R., *et al.* (2007). Neural substrates of awakening probed with optogenetic control of hypocretin neurons. *Nature*, 450(7168), 420-424,PMC6744371.
- Alexandre, C., *et al.* (2013). Control of arousal by the orexin neurons. *Curr Opin Neurobiol*, 23(5), 752-759,PMC3783629.
- Blanco-Centurion, C., *et al.* (2016). Optogenetic activation of melanin-concentrating hormone neurons increases non-rapid eye movement and rapid eye movement sleep during the night in rats. *Eur J Neurosci*, 44(10), 2846-2857,PMC5118149.
- Blanco-Centurion, C., *et al.* (2019). Dynamic Network Activation of Hypothalamic MCH Neurons in REM Sleep and Exploratory Behavior. *J Neurosci*
- Blanco-Centurion, C., *et al.* (2019). Dynamic Network Activation of Hypothalamic MCH Neurons in REM Sleep and Exploratory Behavior. *J Neurosci*, 39(25), 4986-4998,PMC6670248.

- 382 Carlini, V. P., *et al.* (2006). Melanin-concentrating hormone (MCH) reverts the behavioral effects induced by
- 383 inescapable stress. *Peptides*, 27(9), 2300-2306,
- 384 Chemelli, R. M., *et al.* (1999). Narcolepsy in orexin knockout mice: molecular genetics of sleep regulation. *Cell*, 98(4),
- 385 437-451,
- 386 Chou, T. C., *et al.* (2001). Orexin (hypocretin) neurons contain dynorphin. *J Neurosci*, 21(19), RC168,
- 387 Dauvilliers, Y., *et al.* (2014). Cataplexy--clinical aspects, pathophysiology and management strategy. *Nat Rev Neurol*,
- 388 10(7), 386-395,
- 389 Dilsiz, P., *et al.* (2019). MCH neuron dependent reward and feeding. *Neuroendocrinology*
- 390 Gonzalez, J. A., *et al.* (2016). Awake dynamics and brain-wide direct inputs of hypothalamic MCH and orexin networks.
- 391 *Nat Commun*, 7, 11395,PMC4844703.
- 392 Hara, J., *et al.* (2001). Genetic ablation of orexin neurons in mice results in narcolepsy, hypophagia, and obesity.
- 393 *Neuron*, 30(2), 345-354,
- 394 Hishikawa, Y., *et al.* (1968). The nature of sleep attack and other symptoms of narcolepsy. *Electroencephalogr Clin*
- 395 *Neurophysiol*, 24(1), 1-10,
- 396 Hof PR, *et al.* (2000) comparative cytoarchitectonic atlas of the C57BL/6 and 129/Sv mouse brains. Elsevier, Netherland.
- 397 Hung CJ, Ono D, Kilduff TS, Yamanaka A (2019). Dural orexin and MCH neuron-ablated mice display severe sleep
- 398 attacks and cataplexy. *BioRxiv* 880229. doi: <https://doi.org/10.1101/2019.12.17.880229>.
- 399 Hungs, M., *et al.* (2001). Hypocretin/orexin, sleep and narcolepsy. *Bioessays*, 23(5), 397-408,
- 400 Izawa, S., *et al.* (2019). REM sleep-active MCH neurons are involved in forgetting hippocampus-dependent memories.
- 401 *Science*, 365(6459), 1308-1313,
- 402 Jego, S., *et al.* (2013). Optogenetic identification of a rapid eye movement sleep modulatory circuit in the
- 403 hypothalamus. *Nat Neurosci*, 16(11), 1637-1643,PMC4974078.
- 404 Konadhode, R. R., *et al.* (2013). Optogenetic stimulation of MCH neurons increases sleep. *J Neurosci*, 33(25), 10257-
- 405 10263,PMC3685832.
- 406 Kirk, RE (1968) Experimental Design: Procedures for the Behavioral Sciences. Brooks/Cole; Belmont, CA.
- 407 Lin, L., *et al.* (1999). The sleep disorder canine narcolepsy is caused by a mutation in the hypocretin (orexin) receptor 2
- 408 gene. *Cell*, 98(3), 365-376,
- 409 Liu, M., *et al.* (2011). Orexin gene transfer into zona incerta neurons suppresses muscle paralysis in narcoleptic mice. *J*
- 410 *Neurosci*, 31(16), 6028-6040,PMC3634582.
- 411 Liu, M., *et al.* (2016). Orexin gene transfer into the amygdala suppresses both spontaneous and emotion-induced
- 412 cataplexy in orexin-knockout mice. *Eur J Neurosci*, 43(5), 681-688,PMC4783302.
- 413 Luppi, P. H., *et al.* (2011). The neuronal network responsible for paradoxical sleep and its dysfunctions causing
- 414 narcolepsy and rapid eye movement (REM) behavior disorder. *Sleep Med Rev*, 15(3), 153-163,
- 415 Morawska, M., *et al.* (2011). Narcoleptic episodes in orexin-deficient mice are increased by both attractive and aversive
- 416 odors. *Behav Brain Res*, 222(2), 397-400,
- 417 Naganuma, F., *et al.* (2018). Melanin-concentrating hormone neurons contribute to dysregulation of rapid eye
- 418 movement sleep in narcolepsy. *Neurobiol Dis*, 120, 12-20,PMC6195361.
- 419 Nishino, S., *et al.* (2000). Is narcolepsy a REM sleep disorder? Analysis of sleep abnormalities in narcoleptic Dobermans.
- 420 *Neurosci Res*, 38(4), 437-446,
- 421 Oishi, Y., *et al.* (2013). Role of the medial prefrontal cortex in cataplexy. *J Neurosci*, 33(23), 9743-9751,PMC3714797.
- 422 Overeem, S., *et al.* (2001). Narcolepsy: clinical features, new pathophysiologic insights, and future perspectives. *J Clin*
- 423 *Neurophysiol*, 18(2), 78-105,
- 424 Peever, J., *et al.* (2016). Neuroscience: A Distributed Neural Network Controls REM Sleep. *Curr Biol*, 26(1), R34-
- 425 35,PMC5846126.
- 426 Reading, P. (2019). Cataplexy. *Pract Neurol*, 19(1), 21-27,
- 427 Roth, B., *et al.* (1969). REM sleep and NREM sleep in narcolepsy and hypersomnia. *Electroencephalogr Clin*
- 428 *Neurophysiol*, 26(2), 176-182,
- 429 Roy, M., *et al.* (2006). Genetic inactivation of melanin-concentrating hormone receptor subtype 1 (MCHR1) in mice
- 430 exerts anxiolytic-like behavioral effects. *Neuropsychopharmacology*, 31(1), 112-120,
- 431 Scammell, T. E., *et al.* (2009). A consensus definition of cataplexy in mouse models of narcolepsy. *Sleep*, 32(1), 111-
- 432 116,PMC2625315.
- 433 Sun, Y., *et al.* (2019). Activity dynamics of amygdala GABAergic neurons during cataplexy of narcolepsy. *Elife*,
- 434 8PMC6703899.
- 435 Tabuchi, S., *et al.* (2014). Conditional ablation of orexin/hypocretin neurons: a new mouse model for the study of

narcolepsy and orexin system function. *J Neurosci*, 34(19), 6495-6509, PMC4012309.
 Thakkar, M. M., *et al.* (1999). REM sleep enhancement and behavioral cataplexy following orexin (hypocretin)-II
 receptor antisense perfusion in the pontine reticular formation. *Sleep Res Online*, 2(4), 112-120,

440

441

442 **Legends:**

443 **Table 1.** The numbers and percentages of ON (activated) cells during the pre-
 444 cataplexy AW episodes (Pre-C AW) were very similar to those during the AW episodes
 445 not followed by cataplexy (N-C AW). No significant involvement of REM-ON only MCH
 446 neurons in Pre-C AW episodes was observed.

447

448 **Figure 1.** Histology results. orexin⁺ neurons were found in the lateral hypothalamus of
 449 the wild-type MCH-Cre mice (panel A) but were absent in the MCH-Cre^{+/-}/HCRT^{-/-}
 450 narcoleptic mice (panel B). Panel C: illustration of the GRIN lens and miniature camera
 451 installation. Panel D–F: GCaMP6s and MCH expression in the hypothalamus near the
 452 end of the lens. Long arrows: GCaMP6s⁺/MCH⁺ double-labelled neurons. Short
 453 arrowhead: a GCaMP6s⁺/MCH⁻ neuron. CeA: the central nucleus of the amygdala, mfb:
 454 medial forebrain bundle. Scale bar=50 μ m.

455 **Figure Contributions:** Ying Sun performed immunostaining and confocal imaging;
 456 Meng Liu produced the montage.

457 **Figure 2.** Ca²⁺ imaging/transient and synchronized behavioral data. Panel A: Map of 15
 458 cells recorded from Mouse MLCH02. REM-ON cells are green-circled; AW-ON cells are

459 red-circled; REM/AW-ON cells are yellow circled; An unscored cell is white-circled.
460 Panel B: Plots of Ca^{2+} transient of the cells from panel A (thicker red line represents the
461 average), followed by mouse EEG power spectrogram (1 s window size and 0.5 s
462 overlap), EEG/EMG waveforms. N: NREM sleep; R: REM sleep; AW: active waking.
463 Panel C: Average Ca^{2+} transient signal intensity ($\Delta F/F$ Z-scores) of MCH neurons in
464 various states. AW (M): AW during milk exposure; AW (U): AW during coyote urine
465 exposure. **: $p < 0.001$ or * $p < 0.01$ compared to NREM sleep, sleep attack, and cataplexy.
466 Panel D–E: Ca^{2+} transients and EEG/EMG waveforms from Mouse MLCH03 after milk
467 exposure (panel D) and predator odor exposure (panel E). C: cataplexy, SA: sleep
468 attack. Panel F: No significant differences in Ca^{2+} signal intensities (z-scores) and peak
469 frequencies (peaks/cell/min) between Pre-C AW episodes and N-C AW episodes were
470 found.

471 **Figure Contributions:** Ying Sun and Meng Liu performed data analysis; Meng Liu
472 produced the montage.

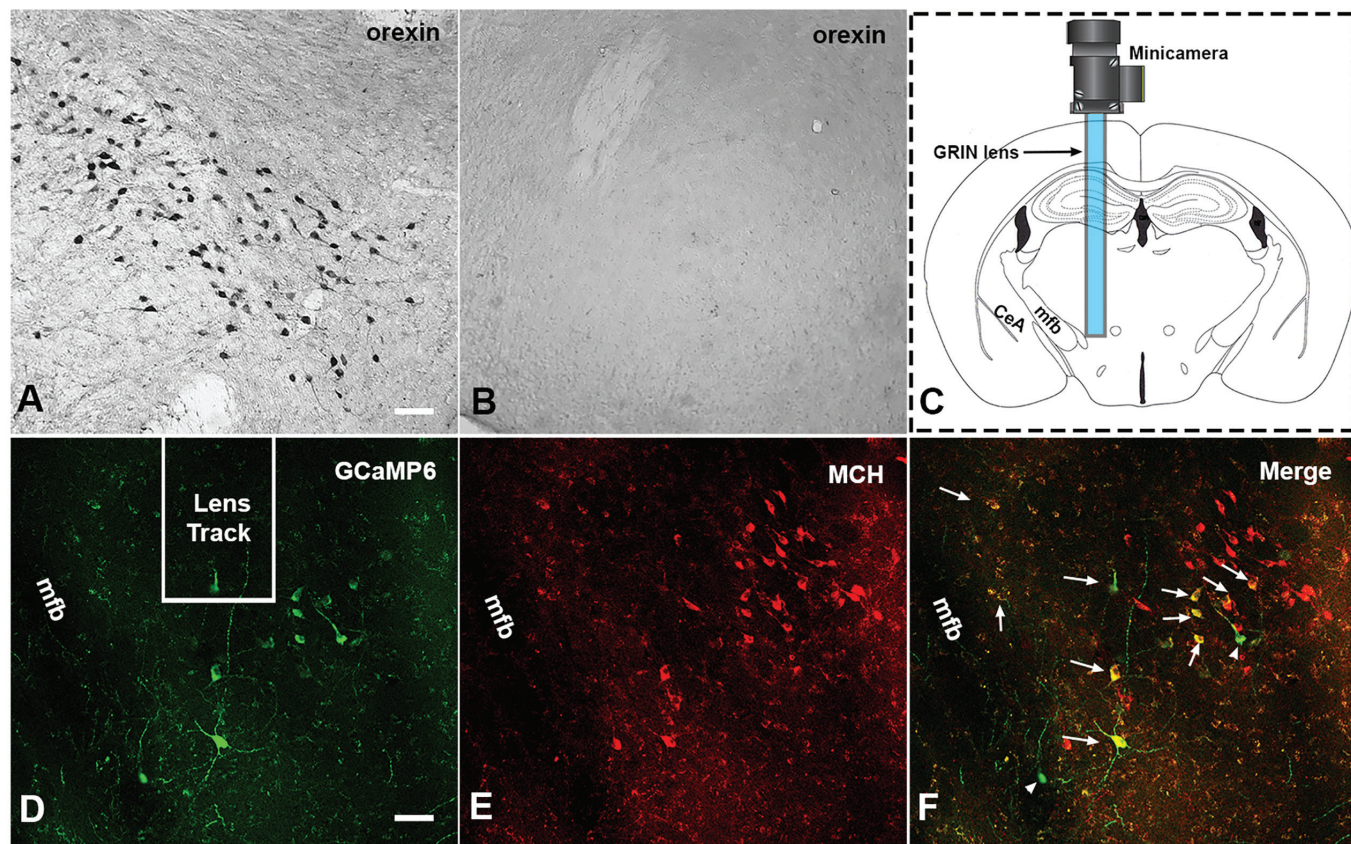
473

474 **Video 1:** The raw calcium movies with synchronized EEG/EMG and animal behavior
475 video during the undisturbed sleep recording shown in Figure 2B (played at 8x speed).

476 **Video 2:** The raw calcium movies with synchronized EEG/EMG and animal behavior
477 video during milk exploring and drinking shown in Figure 2D (played at 8x speed).

478 **Video 3:** The raw calcium movies with synchronized EEG/EMG and animal behavior
479 video during predator odor exposure shown in Figure 2E (played at 8x speed).

480



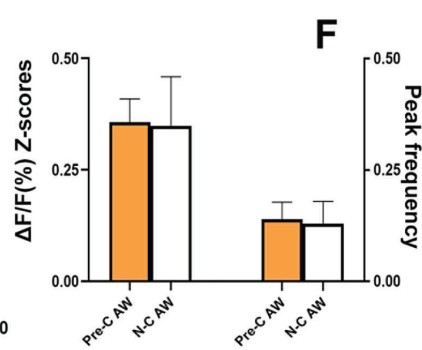
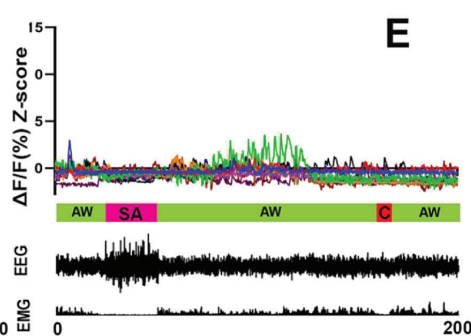
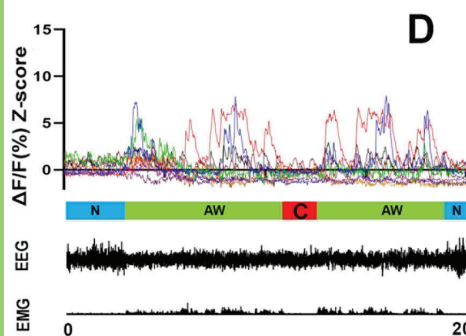
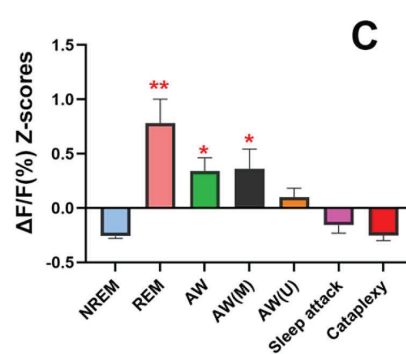
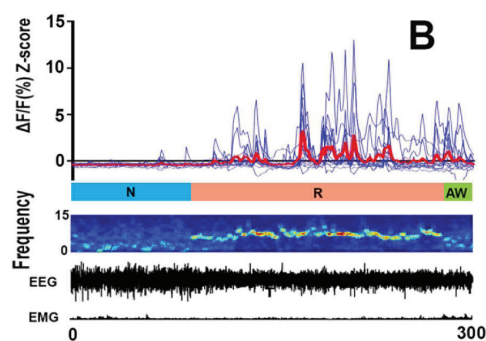
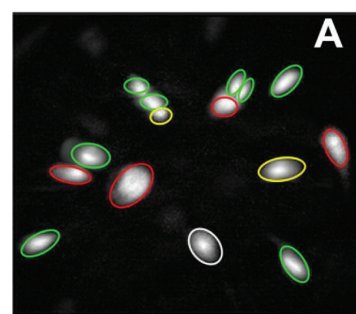


Table 1. Components of ON cells during the Pre-C and N-C AW episodes

| | AW-ON Only | REM-ON Only | REMS-ON REMS/AW-ON | Unscored |
|---------------------------|-------------|-------------|--------------------|-----------|
| N-C AW-ON cells (24) | 14 (58.33%) | 0 (0%) | 10(41.67%) | (0%) |
| Pre-C AW-ON cells (23) | 12(52.17%) | 1 (4.35%) | 9 (39.13) | 1 (4.35%) |